Current Biology, Vol. 14, 225–230, February 3, 2004, ©2004 Elsevier Science Ltd. All rights reserved. DOI 10.1016/j.cub.2004.01.006

Heparan Sulfate Proteoglycan Syndecan Promotes Axonal and Myotube Guidance by Slit/Robo Signaling

Patrick Steigemann, Andreas Molitor, Sonja Fellert, Herbert Jäckle, and Gerd Vorbrüggen*
Abteilung Molekulare Entwicklungsbiologie
Max-Planck-Institut für biophysikalische Chemie
Am Fassberg 11
37077 Göttingen
Germany

Summary

Slit, the ligand for the Roundabout (Robo) receptors [1–3], is secreted from midline cells of the *Drosophila* central nervous system (CNS) [4]. It acts as a short-range repellent that controls midline crossing of axons and allows growth cones to select specific pathways along each side of the midline [1, 3]. In addition, Slit directs the migration of muscle precursors and ventral branches of the tracheal system, showing that it provides long-range activity beyond the limit of the developing CNS [2, 5, 6]. Biochemical studies suggest that guidance activity requires cell-surface heparan sulfate to promote binding of mammalian Slit/Robo homologs [7, 8]. Here, we report that the *Drosophila* homolog of Syndecan (reviewed in [9]), a heparan sulfate proteoglycan (HSPG), is required for proper Slit signaling. We generated *syndecan* (*sdc*) mutations and show that they affect all aspects of Slit activity and cause *robo*-like phenotypes. *sdc* interacts genetically with *robo* and *slit*, and double mutations cause a synergistic strengthening of the single-mutant phenotypes. The results suggest that Syndecan is a necessary component of Slit/Robo signaling and is required in the Slit target cells.

Results and Discussion

Biochemical studies on mammalian Slit revealed that members of this ligand family are capable of binding to the HSPG Glypican, and that the in vitro interaction is sensitive to heparinase III treatment [7]. Furthermore, heparinase III treatment significantly reduced the binding of human Slit2 to Robo1-transfected cells and reduced its biological activity [8]. In contrast to mammals, the *Drosophila* genome contains only a single Slit-coding gene [10], which acts through three receptors: Robo, Robo2, and Robo3 [1, 3]. These receptors are expressed in an overlapping set of axons of the longitudinal tracts that run parallel to the midline of the developing CNS [1, 3]. In order to identify an endogenous HSPG that might participate in Slit signaling, we examined the expression of HSPG-encoding genes by whole-mount in situ hybridization, looking for HSPG encoding genes that are expressed in patterns that include the expression domains of Slit and/or Robo. We observed that *syndecan* (*sdc*), which encodes a conserved transmembrane protein containing a heparan-sulfate-modified extracellular domain [9, 11], shows zygotic patterns overlapping all tissues affected in *slit* mutants and in domains directly adjacent to regions of *slit* expression (Figures 1A–1D).

If Sdc participates in the control of Slit/Robo signaling and is not expressed in Slit-expressing cells, it is likely to be coexpressed with the Robo receptors. Robo2 and Robo3 are expressed in a subset of the Robo-expressing axons [1, 3]. Thus, the anti-Robo antibody labels all axons in which the three *Drosophila* Slit receptors are active. In order to localize the Sdc-expressing cells, we generated Sdc-specific antibodies (see Experimental Procedures) to immunostain embryos in combination with anti-Robo antibodies. Specificity of the antibody staining is indicated by the absence of staining in homozygous *sdc* mutant embryos (data not shown) and by panneural overexpression using the GAL4/UAS system [12]. Panneural Sdc expression was achieved with a UAS-dependent transgene containing an *sdc* cDNA (composed of the translated exons; *sdc-RA* [13]) in response to the *elav*-GAL4-driver (Figure 1E). Figures 1F–1H show coexpression of Sdc and Robo in the longitudinal axons from stage 13 onward. Sdc protein is also expressed across the midline in positions corresponding to the commissural axons that lack Robo (Figures 1F–1H). The heparinase sensitivity of the mammalian Slit/Robo interaction (see above), the molecular nature of Sdc, and its coexpression with Robo (and thus also with Robo2 and Robo3; see above) are consistent with a role of Sdc in Slit signaling.

In order to test this proposal, we generated *sdc* mutants by imprecise excision of a P element inserted in the first intron of the *sdc* gene (Figure 1I). We identified two *sdc* mutations, the alleles sdc^{97} and sdc^{23}, both lacking the first exon, the transcription start site, and parts of the first intron. In contrast to sdc^{97}, the translation start site as well as parts of the signal peptide encoded by the second exon are removed in the sdc^{23} allele (Figure 1I; see legend for details). Both deletion mutants fail to express the *sdc* transcript in all regions of the embryo where transcripts are detected in wild-type embryos. Furthermore, Sdc could not be detected by anti-Sdc antibodies in the mutant embryos (not shown). These findings indicate that the newly generated *sdc* mutants are either strong hypomorphic or amorphic alleles.

Homozygous *sdc* mutants were semilethal and showed identical phenotypes in the CNS and in the muscle pattern (see below). In order to unambiguously demonstrate that the lack of *sdc* activity is responsible for the mutant phenotype observed, we panneurally expressed Sdc-RA using the GAL4/UAS system (see above) in *sdc* mutant individuals. Table 1 shows that the neural phenotype of the mutants was rescued, indicating that the mutant phenotype was caused by the lack of Sdc and that the transgene provides functional Sdc activity.

In order to examine the possible defects in axonal guidance and muscle patterning, we stained *sdc* mutant

*Correspondence: gvorbru@gwdg.de

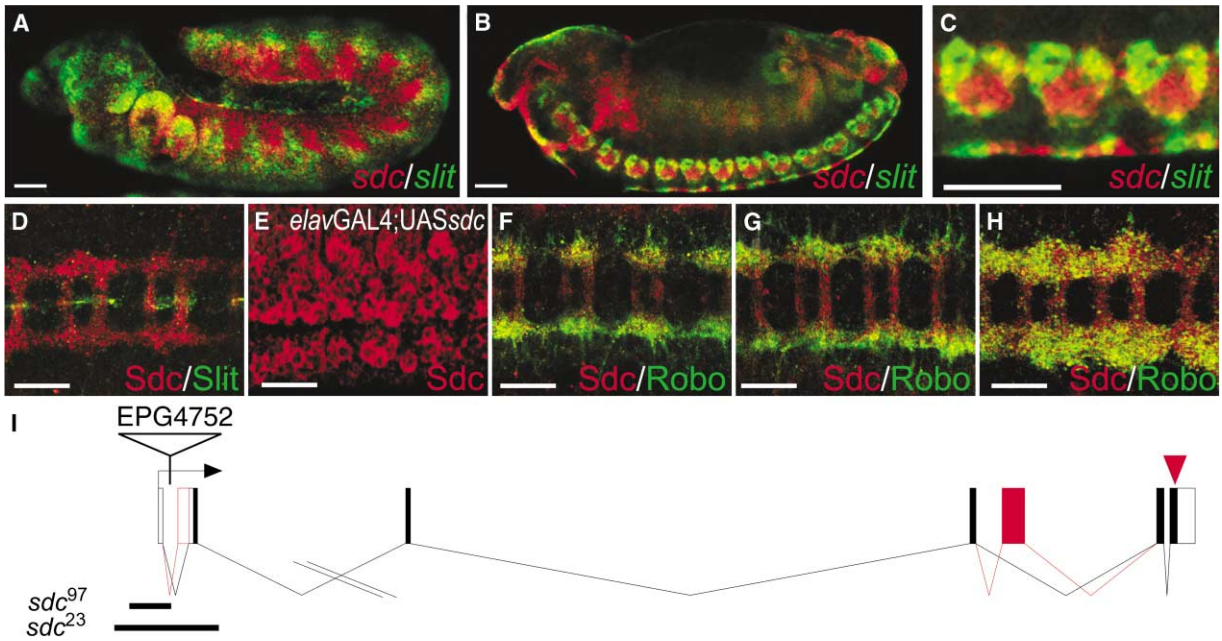

Figure 1. *sdc* and *robo* Are Coexpressed in Domains Adjacent to *slit*

(A) In situ hybridization of a stage 11 wild-type embryo [24] showing *sdc* transcripts in tracheal pits and *slit* transcripts in the surrounding epidermis.

(B and C) At stage 13 [24], *sdc* is expressed in CNS cells neighboring the *slit*-expressing midline glia cells.

(D) Sdc (red) in all axons at stage 14 and Slit (green) in midline cells.

(E) *elav*-GAL4 mediated Sdc (red) overexpression in all postmitotic CNS cells at stage 13 [24].

(F–H) Sdc (red) accumulation in all axons, including the commissures and Robo protein (green), confined to the longitudinal axons ([F], stage 13; [G], stage 14; and [H], stage 16 [24]).

(I) *sdc* encodes two protein variants due to differential splicing; (alternatively used exons in red). Position of the P element insertion (EP G4752), the extent of the deletions of alleles sdc^{97} and sdc^{23}, and the position of the epitope used for antibody production (arrowhead) are marked. In sdc^{97}, the first exon of *sdc* is deleted (nucleotides 1–132 of *sdc*-RA), whereas in sdc^{23} the first and second exons are removed (nucleotides 1–420 of *sdc*-RA). White bar corresponds to 20 μm.

Table 1. Transgene-Dependent Rescue and Genetic Interaction of *sdc*, *slit*, *robo*, and *robo2*

Genotype[f]	Muscles Crossing the Midline per Embryo[a]	Embryos Scored	Inner FasII-Positive Axons Crossing the Midline[b] (%)	Segments Scored	Segments with Additional LT Muscles[c] (%)	Segments Scored
sdc/sdc	1.1	20	17	209	nd	–
sdc/sdc;UASsdc/elav-GAL4	nd	nd	0	253	nd	–
sdc/sdc;UASsdc/sim-GAL4	nd	nd	19	198	nd	–
robo/robo	0.6	20	100[d]	220	nd	–
robo2/robo2	1.6	20	36	198	nd	–
slit/slit	16	20	100[e]	220	nd	–
robo, sdc/robo, sdc	1.4	20	100[d]	220	nd	–
robo2, sdc/robo2, sdc	14	20	100[e]	220	nd	–
robo, sdc/+, sdc	1.1	20	72	198	nd	–
robo2, sdc/+, sdc	3.4	20	47	187	nd	–
slit, sdc/+, sdc	2	20	95	209	nd	–
sdc/+	0	20	0	209	0	204
slit/+	0	20	0.6	462	1	222
slit, +/+, sdc	0	20	3.3	451	3.4	272
perlecan/perlecan	0	20	0	209	nd	–
dally/dally	0	20	0	198	nd	–

[a] Embryo stages 13–15.

[b] Embryo stages 16 and 17, crossing axon bundles as thick as or thicker than normal FasII fascicles.

[c] Embryos stages 16 and 17.

[d] Inner FasII fascicles nearly fused, outer FasII fascicles largely unaffected.

[e] Complete collapse of all FasII fascicles into the midline.

[f] Alleles in Experimental Procedures.

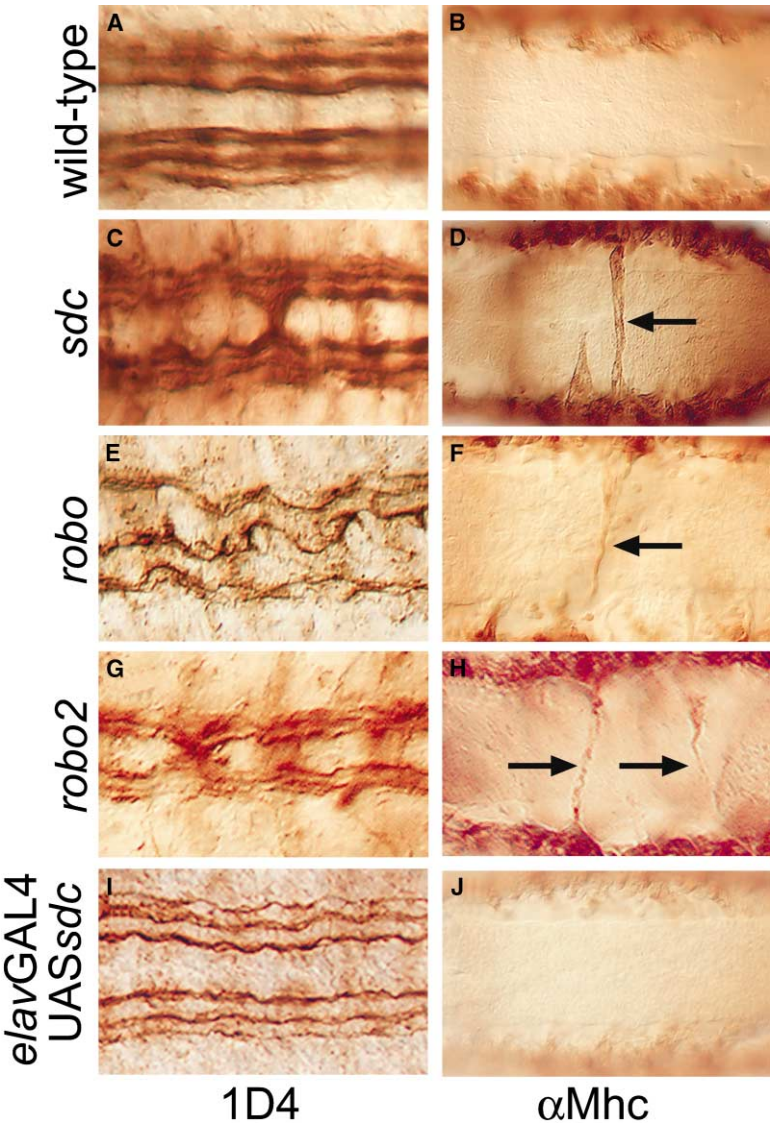

Figure 2. *sdc* Mutants Exhibit a *robo*-like Phenotype

Ventral views of stage 16 [24] embryonic CNS (stained with mAb 1D4 in [A], [C], [E], [G], and [I]) and muscle patterns of stage 14 embryos [24] (stained with anti-Mhc in [B], [D], [F], [H], and [J]).

(A and B) Wild-type embryo showing the three FasII-expressing longitudinal fascicles (A) and the wild-type muscle pattern (B). Note that none of the axon bundles and muscles cross the midline.

(C and D) *sdc* mutant showing that the inner fascicles (C) and single ventral muscles cross the midline ([D], arrow).

(E and F) *robo* mutant showing that the inner fascicles are combined, that they cross and recross the midline (E), and that single ventral muscles cross the midline ([F], arrow).

(G and H) *robo2* mutant show axons (G) and ventral muscles ([H], arrows) crossing the midline.

(I and J) Panneural overexpression (see text) does not affect axon (I) and muscle (J) patterns. For quantitative aspects see Table 1.

embryos with both Fasciclin II (FasII; mAB 1D4) antibodies, which label three longitudinal axon tracts at each side of the midline, and anti-Mhc antibodies, which visualize the muscle pattern. The comparison of *sdc, robo*, and *robo2* mutant phenotypes is shown in Figure 2 and summarized in Table 1. The results show that the lack of *sdc* activity causes phenocopies of *robo* and *robo2* mutants; i.e., it affects both midline guidance of axons and the establishment of the muscle pattern (compare Figures 2D, 2F, and 2H). The defects in CNS axon guidance were strikingly similar to *robo2* mutants but less pronounced than in *robo* mutants (Figures 2C, 2E, and 2G; for details on *robo* mutant phenotypes see [1, 3, 14, 15]). The muscle and CNS phenotypes were also weaker than in *slit* mutants (Figures 3B and 3E), in which signaling through all Robo receptors is impaired.

We next asked whether *sdc* activity participates in the control of *robo* and/or *slit* expression, or vice versa, by examining the strength and patterns of expression of each gene in *sdc*, *robo*, and *slit* mutant embryos. The results showed that there was no crossregulatory effect on gene expression and localization of the proteins (data not shown). In addition, we asked whether panneural overexpression of *sdc* [12] interferes with axonal guidance and the establishment of the muscle patterns. Panneural *sdc* expression was strongly induced in transgene-bearing wild-type embryos (see Figure 1E), but no effect on the FasII-expressing axons (Figure 2I), the commissures (data not shown), and the mytotube pattern (Figures 2J) could be observed. Collectively, the results suggest that in the absence of *sdc* activity, both *slit* and *robo* expression as well as the production and localization of the proteins were not affected, but the effectiveness of the Slit signal is strongly reduced in *sdc* mutants. In addition, panneural *sdc* overexpression does not interfere with Slit signaling.

In order to link embryonic Sdc requirement genetically to Slit/Robo signaling, we next asked whether *sdc* mutations can enhance loss-of-function *slit* and *robo* phenotypes. We found that the number of ventral muscles, which cross the midline dorsal of the CNS in homozygous *sdc* and *robo2* single mutants, is significantly in-

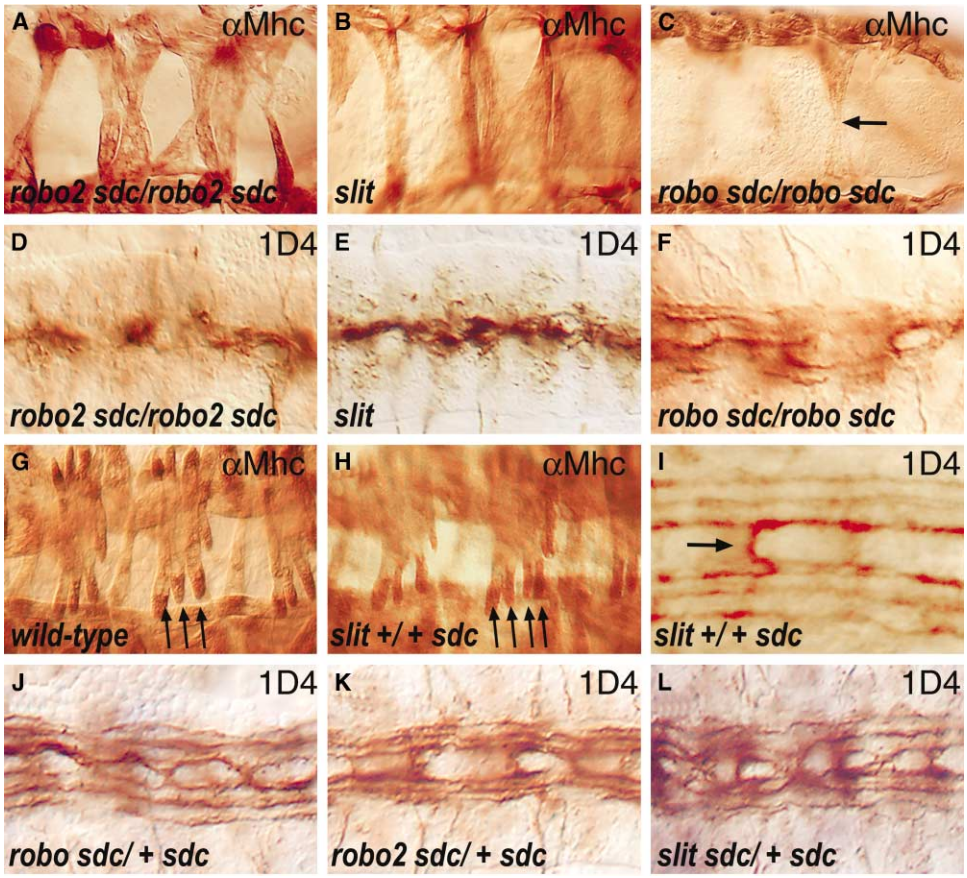

Figure 3. *sdc* Interacts Genetically with *robo, robo2*, and *slit*

(A–C) Ventral views of stage 14 embryos [24] stained with anti-Mhc antibodies. (D–F) and (I–L) Ventral views of stage 16 embryos [24] stained with mAb 1D4. (G and H) Lateral view of stage 16 embryos [24] stained with anti-Mhc antibodies.

(A and D) *robo2, sdc* double mutants show an increased number of ventral muscles that cross the midline, resembling a *slit*-like phenotype (A). Longitudinal axons collapse and form a single fascicle (D).

(B and E) In *slit* mutants most of the ventral muscles cross the midline (B), and all axons of the CNS collapse and form a single fascicle at the midline (E).

(C and F) *robo, sdc* double mutants show a *robo*-like phenotype (crossing muscle marked by arrow in [C]).

(G) In wild-type embryos three longitudinal transverse muscles (LT) are present (arrows).

(H and I) In *sdc slit* transheterozygous embryos additional LT muscles (arrows in [H]) and midline crossings are observed (arrow in [I]).

(J–L) *sdc* mutants lacking one copy of *robo* (J), *robo2* (K), or *slit* (L). Note axonal phenotypes similar to *robo* mutants (midline crossings in nearly every segment). For quantitative aspects see Table 1.

creased in double mutant combinations of *sdc* and *robo2* (Table 1), resulting in a muscle phenotype indistinguishable from *slit* (compare Figures 3A and 3B) and homozygous *robo*, *robo2* double mutants (data not shown). In the CNS, the FasII-expressing longitudinal fascicles of *robo2*, *sdc* double mutants converged into a single thick axon bundle at the ventral midline (Figure 3D), resembling the effects seen with *slit* mutants (Figure 3E). Similar observations were obtained with the mAb BP102 against all CNS axons [16], showing strongly condensed fascicles in *robo2*, *sdc* double mutant embryos (data not shown). The synergistic strengthening of both the muscle and the CNS phenotypes in *robo2*, *sdc* double mutants, which are similar to a weak *slit* mutant phenotype, indicates that only some Slit-derived repellent activity is received along the midline. In contrast to *robo2*, the *robo* mutant phenotype was not significantly enhanced by the simultaneous lack of *sdc* (Figures 3C and 3F; Table 1). The data suggest that Robo can, in part, compensate for the lack of Robo2 and *vice versa* and that Robo is more sensitive to reduced Sdc-dependent Slit activity than Robo2.

The results imply that *sdc*, *slit*, and *robo* are components of the same genetic circuitry. We tested this proposal by genetic means, asking whether the gene activities interact in vivo. Loss of only one copy of *sdc* led to the development of a normal muscle pattern, whereas the simultaneous absence of one copy of both *slit* and *sdc* in *slit*/+, *sdc*/+ double heterozygous embryos caused an increase in the number of longitudinal transverse muscles (compare Figures 3G and 3H; Table 1). Furthermore, the number of FasII-expressing inner fascicles that cross the midline (Figure 3I) is increased (3.3%) as compared to *slit* heterozygous embryos (0.6%; Table 1). More clearly, homozygous *sdc* mutant embryos, which also lack one copy of either *robo*, *robo2*, or *slit*

(Figures 3J–3L), show an enhanced axonal guidance defect with multiple midline crossings of the fascicles (72%, 47%, and 95%, respectively; Table 1), a phenotype very similar to the *robo* mutant. These results establish that Sdc acts in the same genetic circuitry as Slit and the Robo receptor family and represents a critical component of the Slit/Robo signaling pathway.

Axonal expression of Sdc suggests that its activity is required in the Robo-expressing Slit target cells. In order to test this inference, we performed cell-specific rescue experiments by expressing Sdc from either an *elav*-GAL4 or a *sim*-GAL4 driven UAS transgene in Robo-expressing neurons and Slit-expressing midline cells, respectively. The axon guidance defects of the *sdc* mutant were entirely rescued by Sdc expression in neurons, whereas no rescuing activity was seen in response to Sdc expression in midline cells (Table 1). These findings indicate that *sdc* activity is not required for the production and/or secretion of Slit, but in the reception and/or the transmission of the signal in the target cells.

The results present evidence that axonal and myotube guidance in *Drosophila* require the transmembrane HSPG Sdc and that Sdc is an essential component of the Slit/Robo signaling pathway. Our findings are consistent with earlier results showing that heparinase III treatment both weakens the Slit/Robo interaction and the biological effect of Slit signaling in mammalian cell culture [8], but is surprising in the light of the demonstration that mammalian Slit associates with the HSPG Glypican [7]. We therefore also examined *dally* [17] and *perlecan* mutations [18] for potential interaction with Slit/Robo signaling and found no effect (Table 1). In addition, we did not detect any defects in *sdc* mutants reminiscent of impaired Hedgehog, Wingless, or FGF signaling (P.S. and G.V., unpublished data), pathways previously shown to be sensitive to the levels of other HSPGs (reviewed in [19]). Furthermore, Slit signaling in *sdc* mutants is also impaired in other tissues including the tracheal system (P.S. and G.V., unpublished data). Thus, Slit/Robo signaling seems to primarily or even specifically require Sdc among the known *Drosophila* HSPGs. The difference in the nature of the HSPG that interacts with Slit in *Drosophila* and mammals may either reflect a species-dependent difference or a difference between the in vivo situation shown here and the previously published in vitro analysis. Other remarkable results are the spatially restricted requirement for Sdc as suggested by its expression domains adjacent to Slit-expressing cells and the finding that no defects, other than those related to Slit/Robo signaling, could be observed. Furthermore, overexpression of Sdc in the Slit target tissue did not interfere with proper Slit signaling. This result and the finding that overexpression of Sdc in the Slit-secreting midline glia cells also has no effect on axonal pathfinding and myotube guidance (data not shown) make it unlikely that Sdc functions as a simple ligand gatherer of soluble Slit. In addition, the rescue and protein localization studies indicate that Sdc functions in the target tissue and not in the Slit-secreting cells and acts in a Robo receptor-dependent manner. Sdc could, therefore, function to stabilize and/or transduce the Slit signal. Sdc may act as a coreceptor that presents Slit to Robo receptors or stabilizes the ligand receptor complex. Alternatively, signaling across the cell membrane might involve the Sdc-dependent organization of microdomains within the target cell membrane as has recently been proposed for vertebrate Sdc proteins (reviewed in [9]).

Experimental Procedures

Fly Strains

Wild-type Oregon R and *elav*-GAL4 were obtained from the Bloomington stock center. *robo*$^{Q1\text{-}15}$ and *slit*^{2} mutants were kindly provided by Barry Dickson, the *sim*-Gal4 and the *leak*^{1} (*robo2*) stock by Christian Klämbt, *dally*$^{\Delta P\text{-}527}$, *trol*^{Null} *(perlecan)* by Aaron Vogt, and the EP G4752 by Ulrich Schäfer. EP G4752 was used to generate *sdc* mutants by mobilizing the P element insertion [20]. Subsequent analyses were according to standard procedures described earlier [18].

Transgenic Flies

The EST LD08230 (corresponds to the *sdc*-RA transcript [13]) was cloned into pUAST [12], and transgenic lines were generated [21].

Staining of Embryos

Whole-mount fluorescent in situ hybridization and antibody staining were performed as described [22, 23]. Rabbit anti-Mhc (1:2000; kindly provided by D. Kiehart) and mouse mAB 1D4 (1:15; Developmental Studies Hybridoma Bank; DSHB) and anti-Slit (1:5; DSHB) and anti-Robo (1:10; DSHB) were used as primary antibodies, goat anti-mouse and anti-rabbit (coupled to biotin, 1:500; Vectastain or with Alexa 488 or 546 1:500; Molecular Probes) were used as secondary antibodies. Images were taken with the Zeiss Axiophot and laser-scanning microscopes.

Antibodies

Polyclonal anti-Sdc antibodies against the peptide NNSYAKNANN REFYA (corresponding to carboxy-terminal 15 amino acids of the intracellular portion of the protein [13]) were raised in rabbits and affinity purified. Specificity was demonstrated by lack of anti-Sdc antibody staining in *sdc* mutant embryos and detection of ectopic Sdc expression sites when induced in response to the GAL4/UAS system [12] (see text).

Acknowledgments

We thank our colleagues in the lab for their various contributions and critical discussions, Berktan Akyildiz for help during the characterization of the *sdc* mutants, G. Dowe for sequencing, and U. Jahns-Meyer for transformations. We are grateful to Barry Dickson, Stefan Baumgartner, Christian Klämbt, and Christos Samakovlis for fly stocks. This work was supported by the Max-Planck-Society (H.J.) and the SFB271 and the Graduiertenkolleg "Molekulare Genetik der Entwicklung" of the DFG (G.V.).

Received: October 23, 2003
Revised: December 16, 2003
Accepted: December 16, 2003
Published online: January 12, 2004

References

1. Rajagopalan, S., Vivancos, V., Nicolas, E., and Dickson, B.J. (2000). Selecting a longitudinal pathway: Robo receptors specify the lateral position of axons in the *Drosophila* CNS. Cell *103*, 1033–1045.
2. Kidd, T., Bland, K.S., and Goodman, C.S. (1999). Slit is the midline repellent for the robo receptor in *Drosophila*. Cell *96*, 785–794.
3. Simpson, J.H., Bland, K.S., Fetter, R.D., and Goodman, C.S. (2000). Short-range and long-range guidance by Slit and its Robo receptors: a combinatorial code of Robo receptors controls lateral position. Cell *103*, 1019–1032.
4. Rothberg, J.M., Jacobs, J.R., Goodman, C.S., and Artavanis-Tsakonas, S. (1990). slit: an extracellular protein necessary for

development of midline glia and commissural axon pathways contains both EGF and LRR domains. Genes Dev. *4*, 2169–2187.
5. Kramer, S.G., Kidd, T., Simpson, J.H., and Goodman, C.S. (2001). Switching repulsion to attraction: changing responses to slit during transition in mesoderm migration. Science *292*, 737–740.
6. Englund, C., Steneberg, P., Falileeva, L., Xylourgidis, N., and Samakovlis, C. (2002). Attractive and repulsive functions of Slit are mediated by different receptors in the Drosophila trachea. Development *129*, 4941–4951.
7. Liang, Y., Annan, R.S., Carr, S.A., Popp, S., Mevissen, M., Margolis, R.K., and Margolis, R.U. (1999). Mammalian homologues of the Drosophila slit protein are ligands of the heparan sulfate proteoglycan glypican-1 in brain. J. Biol. Chem. *274*, 17885–17892.
8. Hu, H. (2001). Cell-surface heparan sulfate is involved in the repulsive guidance activities of Slit2 protein. Nat. Neurosci. *4*, 695–701.
9. Couchman, J.R. (2003). Syndecans: proteoglycan regulators of cell-surface microdomains? Nat. Rev. Mol. Cell Bio. *4*, 926–937.
10. Rothberg, J.M., Hartley, D.A., Walther, Z., and Artavanis-Tsakonas, S. (1988). slit: an EGF-homologous locus of D. melanogaster involved in the development of the embryonic central nervous system. Cell *55*, 1047–1059.
11. Spring, J., Paine-Saunders, S.E., Hynes, R.O., and Bernfield, M. (1994). *Drosophila syndecan*: conservation of a cell-surface heparan sulfate proteoglycan. Proc. Natl. Acad. Sci. USA *91*, 3334–3338.
12. Brand, A.H., and Perrimon, N. (1993). Targeted gene expression as a means of altering cell fates and generating dominant phenotypes. Development *118*, 401–415.
13. Adams, M.D., Celniker, S.E., Holt, R.A., Evans, C.A., Gocayne, J.D., Amanatides, P.G., Scherer, S.E., Li, P.W., Hoskins, R.A., Galle, R.F., et al. (2000). The genome sequence of Drosophila melanogaster. Science *287*, 2185–2195.
14. Rajagopalan, S., Nicolas, E., Vivancos, V., Berger, J., and Dickson, B.J. (2000). Crossing the midline: roles and regulation of Robo receptors. Neuron *28*, 767–777.
15. Simpson, J.H., Kidd, T., Bland, K.S., and Goodman, C.S. (2000). Short-range and long-range guidance by slit and its Robo receptors. Robo and Robo2 play distinct roles in midline guidance. Neuron *28*, 753–766.
16. Seeger, M., Tear, G., Ferres-Marco, D., and Goodman, C.S. (1993). Mutations affecting growth cone guidance in *Drosophila*: genes necessary for guidance toward or away from the midline. Neuron *10*, 409–426.
17. Nakato, H., Futch, T.A., and Selleck, S.B. (1995). The division abnormally delayed (dally) gene: a putative integral membrane proteoglycan required for cell division patterning during postembryonic development of the nervous system in Drosophila. Development *121*, 3687–3702.
18. Voigt, A., Pflanz, R., Schäfer, U., and Jäckle, H. (2002). Perlecan participates in proliferation activation of quiescent Drosophila neuroblasts. Dev. Dyn. *224*, 403–412.
19. Perrimon, N., and Bernfield, M. (2000). Specificities of heparan sulphate proteoglycans in developmental processes. Nature *404*, 725–728.
20. Robertson, H.M., Preston, C.R., Phillis, R.W., Johnson-Schlitz, D.M., Benz, W.K., and Engels, W.R. (1988). A stable genomic source of P element transposase in Drosophila melanogaster. Genetics *118*, 461–470.
21. Rubin, G.M., and Spradling, A.C. (1982). Genetic transformation of *Drosophila* with transposable element vectors. Science *218*, 348–353.
22. Zaffran, S., Kuchler, A., Lee, H.H., and Frasch, M. (2001). biniou (FoxF), a central component in a regulatory network controlling visceral mesoderm development and midgut morphogenesis in Drosophila. Genes Dev. *15*, 2900–2915.
23. Vorbrüggen, G., and Jäckle, H. (1997). Epidermal muscle attachment site-specific target gene expression and interference with myotube guidance in response to ectopic stripe expression in the developing Drosophila epidermis. Proc. Natl. Acad. Sci. USA *94*, 8606–8611.
24. Campos-Ortega, J.A., and Hartenstein, V. (1985). The Embryonic Development of *Drosophila melanogaster*. (Berlin: Springer-Verlag).